Phenylene Ring Dynamics in Solid Polycarbonate: An Extensive Probe by Carbon-13 Solid-State NMR Line-Shape Studies at Two Field Strengths

Ajoy K. Roy and Alan Anthony Jones

Department of Chemistry, Clark University, Worcester, Massachusetts 01610

Paul T. Inglefield*

Department of Chemistry, College of the Holy Cross, Worcester, Massachusetts 01610.
Received November 13, 1985

ABSTRACT: An analysis of carbon-13 chemical shift anisotropy (CSA) line shapes at two field strengths is carried out to probe the detailed nature of phenylene ring dynamics in the glassy polycarbonate of bisphenol A. The phenylene group in this polymer undergoes two types of motion simultaneously, both about the C_1C_4 axis. The primary motion is large-angle jumps between two sites whereas the secondary motion involves restricted rotational diffusion over limited angular amplitude. In the first category, the jumps from one minimum to the second occur over an angular range around each minimum associated with the range of restricted rotation. A simultaneous model with an inhomogeneous distribution of correlation times appears to be the best description for the composite motional process. The inhomogeneous distribution is described by a Williams–Watts fractional exponential correlation function and corresponds to a distribution of rates corresponding to different spatial positions in the polymer matrix. The correlation function is described by τ_p, the central correlation time, and α, the breadth parameter for the distribution. An apparent activation energy of 50 kJ/mol, found by an Arrhenius analysis of τ_p's, is in agreement with the values obtained from a relaxation map constructed from rates for proton relaxation minima, CSA line-shape collapse, dielectric loss maxima, and dynamic mechanical loss maxima. A value of 0.154 for the fractional exponent indicates a broad distribution of jump rates for polycarbonate and is consistent with defect diffusion past a distribution of barrier heights. Such diffusion has been proposed as the basic process behind the jumps in a motional model involving conformational interchange between a defect cis–trans conformation of the carbonate unit and neighboring trans–trans conformations.

Introduction

NMR line-shape experiments[1,2] have recently yielded new insights into the dynamics of the polycarbonates of bisphenol A (BPA-PC). To date, the solid-state NMR line-shape experiments[1,2] have defined the geometry of the dominant motions in this polymer, which supplemented the frequency information supplied by dielectric[3] and dynamic mechanical[4] experiments. The two major motional processes are (i) restricted rotational diffusion over limited angular amplitude around the C_1C_4 axis and (ii) π flips between two potential minima around the same axis, with the π flips constituting the primary motion. This geometric information has led to a new motional proposal[5] which attempts to reconcile NMR, dielectric, and dynamic mechanical data. To date, the analysis of the temporal aspects of the NMR line-shape data has been somewhat simplistic and incomplete. In this paper, new data are added and a more rigorous interpretation is pursued to improve the description of the time scale of motion as seen through NMR line shapes.

To review the situation at hand, first consider the chemical shift anisotropy (CSA) study,[1] which suffers from an interpretational inadequacy since the two important motions were treated sequentially. The secondary motion was treated first since it was always assumed to be in the rapid limit. A single-exponential correlation time with an Arrhenius form is then employed to account for the temperature dependence of the π flips.[1,6] The effects of the secondary motion were combined with the primary motion by using partially averaged parameters as the input basis for the primary motion. Problems were encountered with the simulation of the spectrum at 0 °C, the temperature at which both processes make comparable contributions to the line-shape narrowing. At this temperature, the maximum intensity of the theoretical line shape is displaced from the observed one.[1]

To avoid this difficulty, a new model[7] which allows for simultaneous treatment of both motions has been applied to the same set of CSA data. The problem in fitting the 0 °C data in the sequential treatment disappears in this simultaneous treatment. The interpretation for primary motion is also changed in the sense that in the simultaneous treatment jumps over a limited range around each minimum are allowed in addition to exact π flips. The simultaneous treatment also yields a more reasonable temperature dependence for the apparent simple harmonic nature of the secondary motion. However, one problem reported in the earlier CSA paper[1] still remains unaddressed.

The earlier CSA data at 22.6-MHz field strength were analyzed on the basis of a single-exponential correlation function. The Arrhenius analysis of the correlation times yielded an apparent activation energy of 11 kJ/mol. The simultaneous treatment activation energy is 26 kJ/mol. The earlier CSA report[1] also showed an activation energy of 48 kJ/mol, obtained from a linear least-squares analysis of a relaxation map which included spin–lattice relaxation data, dielectric data, and dynamic mechanical data. The phenylene proton T_1 and $T_{1\rho}$ data presented in the same earlier report could only be analyzed on the basis of a broad distribution of exponential correlation times, which corresponds to a fractional exponential correlation function with an exponent near 0.18. Thus there is a great deal of discrepancy between activation energies from two sets of analyses: 11 vs. 48 kJ/mol and the use of a single exponential vs. a broad distribution. The discrepancy points to the inadequacy of the kinetic treatment used for the line-shape data and is an indication of the existence of a distribution of correlation times in the dynamics. The simultaneous value of 26 kJ/mol is probably an improvement but hardly a total resolution. The earlier CSA data at 22.6 MHz represented a limited data set and as

0024-9297/86/2219-1356$01.50/0

such it did not warrant use of a correlation function based on a distribution of correlation times. It is, therefore, necessary that the CSA data base be expanded by acquiring line shapes at another field, preferably a higher one, and that a detailed analysis be carried out in order to reach a better agreement between different data sets.

The Ngai formalism[8-10] for the stretched exponential correlation function used in the earlier T_1 and $T_{1\rho}$ analyses[1] assumes a homogeneous distribution of correlation times where each phenylene group motion follows essentially the same nonexponential decaying process as opposed to an inhomogeneous distribution where spatially separated groups reorient with different time constants. In the case of proton T_1 and $T_{1\rho}$ data, the presence of an efficient spin-diffusion mechanism removes the difference between the two types of distributions. This is however not the case with carbon-13 T_1 and $T_{1\rho}$ data, where a T_1 dispersion can be observed because of weak spin diffusion. A dispersion of spin–lattice relaxation times, in general, indicates the presence of an inhomogeneous distribution, and phenylene carbon-13 $T_{1\rho}$ dispersions were observed by Schaefer et al.[11] for BPA-PC. Line-shape studies offer the possibility of confirming this characteristic of the correlation function.[12] Deuterium NMR[2] has already shown promise in this direction, although a detailed analysis is not yet available. In this context, it appears that if the existing CSA data base at 22.6 MHz is augmented by adding data at a higher field where changes in line-shape features are more pronounced, it might be possible to quantitatively distinguish between a single exponential and a distribution, and in the case of a distribution, between inhomogeneous and homogeneous.[12]

Experimental Section

The same BPA-PC sample with single-site carbon-13 enrichment (<90%) at one of the two phenylene carbons ortho to the carbonate is employed here as was used in an earlier study.[1] The FID's were acquired by using a single pulse with high-power decoupling on a Bruker WM-250 with the Doty solids accessory. A sufficient number of scans were taken at each temperature to ensure a good signal-to-noise ratio. The Fourier-transformed spectra are corrected for a contribution from the background, by using a subtraction scheme; i.e., spectra for the blank probe were obtained under the same conditions, using the same number of scans, and subtracted from the uncorrected spectra. The corrected line shapes at different temperatures were assigned a standard reference following the approach outlined before.[1] CSA line shapes at 62.9 MHz are shown in Figure 1 as a function of temperature. The CSA data on 22.6 MHz are reported in ref 1.

Interpretation

The principal axis system for the CSA tensor of aromatic carbons, as reported for benzene,[13] is oriented with the σ_{11} axis parallel to the C–H bond and the σ_{33} axis perpendicular to the ring plane. The σ_{22} axis is in the ring plane perpendicular to the C–H bond. Low-temperature (less than −140 °C) line shapes at both frequencies were then matched with theoretical spectra generated on the basis of the Bloembergen–Rowland equation.[14] The principal shielding tensor values used to obtain fits at both frequencies are $\sigma_{11} = -15$, $\sigma_{22} = 51$, and $\sigma_{33} = 171$ ppm on the CS_2 scale. These values are in good agreement with the ones reported earlier.[1] These principal values lead to an isotropic chemical shift of 69 ppm, which compares favorably with the observed chemical shift in solution of 72.5 ppm.

Simultaneous Model with a Single Correlation Time. This model[7] provided the best description of the CSA line-shape data at a single frequency and as such it can be considered first in the attempt to interpret the data at two field strengths. In this model, the multisite exchange formalism developed independently by Wemmer[6,15] and Mehring[13] is employed. It allows for all possible transitions with equal probability for a series of sites chosen to emulate large-angle jumps over a range around exact π flips, superimposed on low-amplitude libration both about the C_1C_4 axis of the phenylene ring. The line-shape equation for multisite exchange used for CSA line shapes has been described elsewhere.[1,7] Both two-site jump and simultaneous models make use of the multisite formalism. The two-site jump model includes only the primary motion. The simultaneous model, on the other hand, treats both motions. For BPA-PC, it is important to meet one restriction, i.e., using a correlation time that will treat the secondary motion, namely oscillation or libration in the rapid limit. With two rates, one for each process is conceivable though computationally difficult.

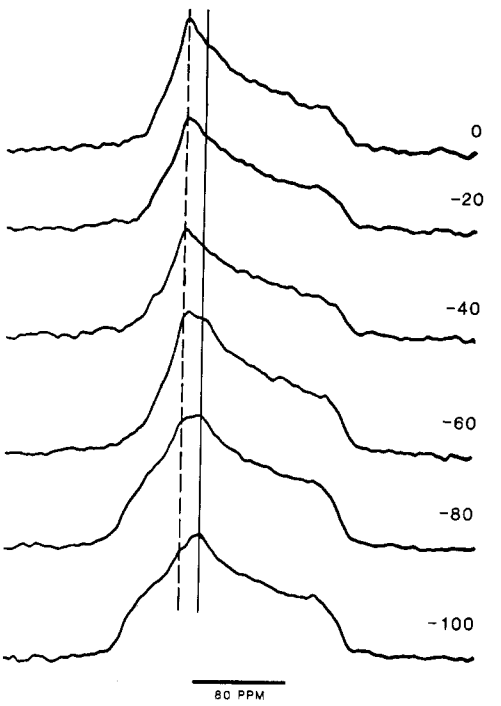

Figure 1. Variable-temperature carbon-13 CSA line shapes at 62.9 MHz. The solid vertical line indicates the position of the maximum in the rigid line shape corresponding to σ_{22}. The dashed vertical line indicates the position of the maximum in the high-temperature, motionally averaged spectra. At the intermediate temperatures of −60 and −80 °C, two maxima corresponding to the two lines are observed, which is indicative of an inhomogeneous distribution.

Whereas 22.6-MHz data were not difficult to simulate with this model, problems were encountered in fitting 62.9-MHz data, mainly the low-temperature ones as shown in parts a and d of Figure 2 for data at −80 and −60 °C. Here the line shapes in the slow-to-intermediate regime play the crucial role in determining the best description of the motion; and the inability to obtain a good match to both frequency sets points to the inadequacy of the treatment of the large-amplitude jumps by a single correlation time.

Inhomogeneous vs. Homogeneous Distribution. In view of the failure of the single correlation time model, a simulation of the data using both distributional models is attempted. The appearance of the spectra shown in Figure 1 is qualitatively indicative of an inhomogeneous distribution. For a simple two-line collapse, Garroway[12] showed the characteristic of a broad inhomogeneous correlation function is an intermediate three-line spectrum. Two of the three lines correspond to the position of the two lines in the absence of exchange. The third line

position corresponds to that of the rapid-exchange limit. Thus the intermediate three-line spectrum consists of two lines corresponding to the precollapse positions and a third line corresponding to the complete collapse position. In the spectra of Figure 1 a solid line is drawn through all spectra for the σ_{22} shift position of the rigid line shape. A dashed line is then drawn through all spectra corresponding to the high-temperature limit resulting from the motional averaging of σ_{11} and σ_{22}. This dashed line is based on the maximum of the high-temperature line shape. At the intermediate temperatures of −60 and −80 °C, maxima are present which correspond to both high-temperature and low-temperature limits, the solid and dashed lines. This feature is qualitatively indicative of an inhomogeneous distribution, and now a quantitative analysis centering on these intermediate temperatures is pursued.

Specifically the calculations will be restricted to the intermediate rate regime where correlation times for the primary motion are slow enough to cause distinctive changes in the maximum intensity area of the line shapes and where secondary motion is not as important. Since the distributions are concerned with the primary motion, a simple two-site jump model is used for preliminary calculation.

The distribution formalism, in general, makes use of a fractional exponential correlation function. The commonly used Williams–Watts expression[16] is

$$\phi(t) = \exp(-t/\tau_p)^\alpha \quad (1)$$

where τ_p is the center correlation time, and α, the breadth parameter. Smaller α's are associated with broader distributions. As shown by Kaplan and Garroway[12] eq 1 can be recast in the form

$$\phi(t) = \int_0^\infty d\tau\ \rho_\alpha(\tau) \exp(-t/\tau) = \int_{-\infty}^{\infty} d(\log \tau) G(\log \tau) \exp(-t/\tau) \quad (2)$$

Instead of the continuous distribution of eq 2, $\phi(t)$ can be represented as a discrete sum.

$$\phi(t) = \sum_j p_j \exp(-t/\tau_j) \quad (3)$$

with a normalization condition given by $\phi(0) = 1 = \sum_j p_j$:

$$p_j = G(\log \tau_j)[\log (\tau_{j+1}/\tau_j)] \quad (4)$$

where by the definition in eq 2

$$G(\log \tau) = \tau \rho_\alpha(\tau)/\log e \quad (5)$$

Montroll and Bendler[17] reported a lognormal expansion of $\rho_\alpha(\tau)$. Later on, Bendler and Shlesinger[18] showed that this series expansion (eq 60b, ref 17) suffers from poor convergence and lack of normalization. They found eq 59 of ref 17 to be superior in both respects. The same series expansion of $\rho_\alpha(\tau)$ as recast by Bendler et al.[18] (eq 51, ref 18) and shown below, is used in our calculation.

$$\rho_\alpha(\tau) = \frac{\alpha}{\tau_p}(\tau/\tau_p)^{\alpha-1} \exp[-(\tau/\tau_p)^\alpha] \times [1 - \alpha F_2 + \alpha^2 F_3 - \alpha^3 F_4 + \alpha^4 F_5 - ...] \quad (6)$$

where

$$F_2 = U_2(1 - \mu^{-\alpha})$$

$$F_3 = U_3(1 - 3\mu^{-\alpha} + \mu^{-2\alpha})$$

$$F_4 = U_4(1 - 7\mu^{-\alpha} + 6\mu^{-2\alpha} - \mu^{-3\alpha})$$

$$F_5 = U_5(1 - 15\mu^{-\alpha} + 25\mu^{-2\alpha} - 10\mu^{-3\alpha} + \mu^{-4\alpha})$$

and $U_2 = 0.577\,216\,65$, $U_3 = -0.655\,877\,5$, $U_4 = -0.042\,003\,28$, $U_5 = 0.166\,538\,57$, and $\mu = \tau_p/\tau$.

Using the correlation function expression of eq 3, Kaplan et al. developed the final line-shape expression for a homogeneous distribution for a two-site exchange process (eq 22, ref 12). In our calculation, the same expression is extended to a polycrystalline type line shape.

For the inhomogeneous distribution, the same Wemmer line-shape expression[6] for multisite exchange is employed with a distribution of correlation times instead of a single correlation time. Each correlation time makes its own contribution toward the total line-shape collapse and the contribution in each case is weighted according to the distribution embodied in eq 3. In essence, the mathematical difference between the homogeneous and inhomogeneous treatments is that in the inhomogeneous case we have a set of uncoupled equations corresponding to the magnetization sites evolving under exchange independently without regard to state of the magnetization at other sites and for the homogeneous case the exchange of each site is coupled with the overall magnetization from all sites.

To save computer time, the following scheme was adopted. At the longer correlation time end, some point is reached when the line shape approaches the rigid limit; i.e., τ_j becomes so long that the jump for such a long τ_j does not cause line-shape collapse and essentially the rigid-case line shape results. There can still be some τ_j's left which are longer than this τ_j and their weightings must be considered. It is not necessary to repeat the line-shape calculation for these long τ's since the rigid limit has already been reached. Instead, the weightings for these τ's are combined with the weighting for this τ_j. The same time-saving scheme can be adopted for τ's at the shorter τ end where at one point the line shape reaches the rapid limit and further decrease in the value of τ leads to no additional narrowing.

For our calculation, 57 τ's were used, 28 on each side of τ_p spanning 28 decades of time (eq 4 and 5). Two τ's thus cover one decade, in accordance with the approach adopted by Kaplan et al.[12] An α value of near 0.16 is suitable for comparing both types of distributions. Comparisons focused on the 62.9-MHz data, which are sensitive enough to force a choice between the two distributions.

Calculations were restricted to the spectra at −80, −60, and −40 °C, which show distinctive temperature-dependent changes in the maximum-intensity area. Figure 2b,e (homogeneous) and Figure 2c,f (inhomogeneous) show the theoretical simulations with appropriate τ_p's for the experimental data at −80 and −60 °C. The distinctive dual-peak nature of the top part of the spectra can only be simulated by using the inhomogeneous distribution, which is at once evident from the figures for data at −80 and −60 °C. A homogeneous distribution results in featureless broadening as can be seen from the figure. These findings are thus in agreement with similar observations based on deuterium spectra[2] and we therefore concentrate the remaining interpretational efforts on the inhomogeneous distribution.

Simultaneous Model with an Inhomogeneous Distribution. For an improved interpretation, the simultaneous model is combined with an inhomogeneous distribution so that both motional processes can be treated at the same time. Some precautions are necessary. For BPA-PC, the secondary motion is always to be treated in the rapid limit. This condition is not met with for some of the longer τ's at the long-τ end, especially when τ_p is long, i.e., when slow-rate-regime line shapes are encountered. Again the following reasonable approximation is pursued. In doing calculation for the entire distribution,

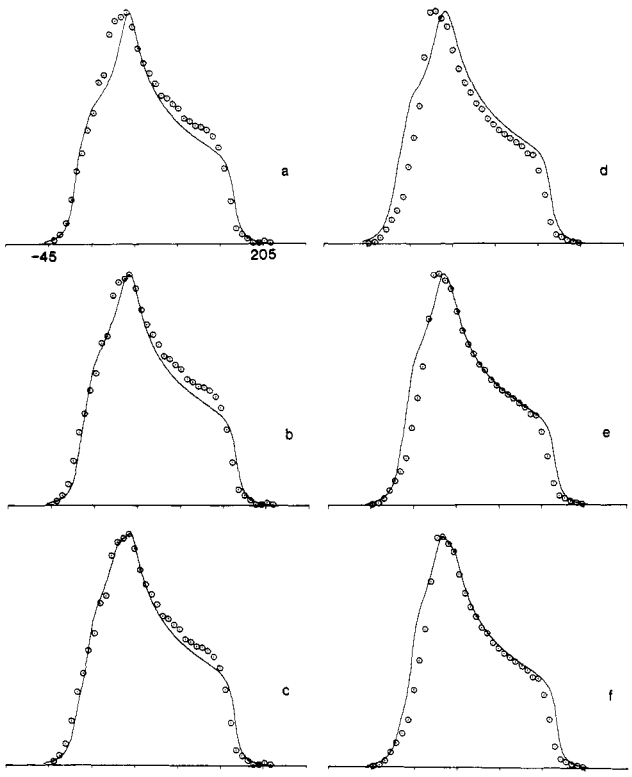

Figure 2. Comparison of simultaneous (a and d), two-site homogeneous (b and e), and two-site inhomogeneous (c and f) treatments for simulation of 62.9-MHz CSA data at −80 and −60 °C. In each case, the solid line represents the best simulation of the experimental data (O). (a) $\tau = 8.0 \times 10^{-4}$ s; (b) $\tau_p = 2.0 \times 10^{-7}$ s, $\alpha = 0.16$; (c) $\tau_p = 5.5 \times 10^{-3}$ s, $\alpha = 0.16$; (d) $\tau = 2.6 \times 10^{-4}$ s; (e) $\tau_p = 1.0 \times 10^{-8}$ s, $\alpha = 0.16$; (f) $\tau_p = 2.6 \times 10^{-4}$ s, $\alpha = 0.16$.

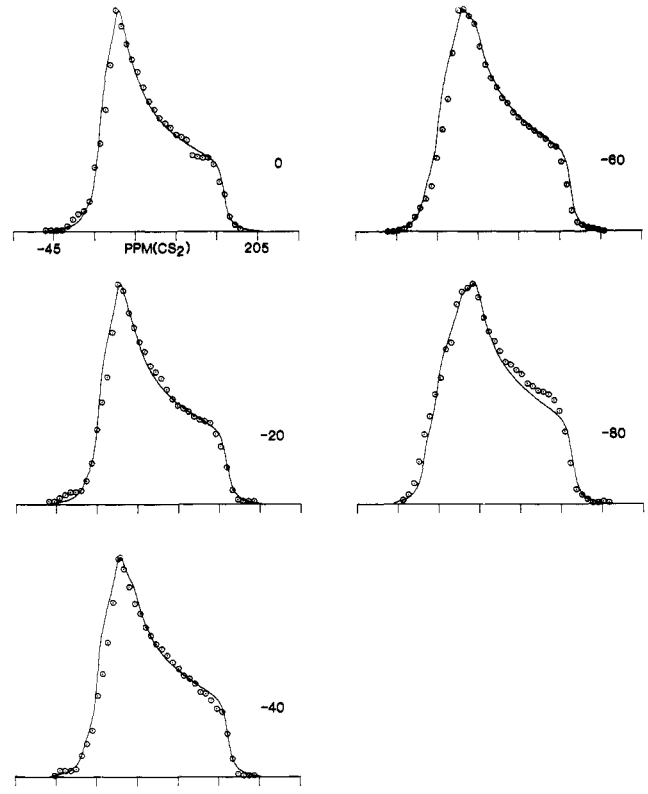

Figure 3. The solid lines are simulations of the 62.9-MHz CSA data (O) at several temperatures.

a point is reached when the τ_j no longer treat the secondary motion in the rapid limit. Again it is also possible that for that particular τ_j and all larger τ's, the rigid line shape is already achieved with respect to the large-amplitude jumps. This means simultaneous jump calculations are not necessary for the τ's in question; instead, line-shape intensities due to oscillation are calculated over an adequate number of frequency points to cover the entire spectrum by applying this motion alone to the rigid tensor principal values. The intensities are then multiplied by the sum of weightings for those long τ's, yielding a line-shape contribution for the long τ's part. For the remaining shorter τ's, the jump calculation is important. The simultaneous model is therefore applied for these remaining τ's, with the intensities obtained by summing up contributions for each τ according to the weighting factor given by the stretched exponential form. We then add up intensities for both the long and short correlation time parts to get the final line shape for the entire distribution. Again 57 τ's are employed.

Since the CSA line shape data do not seem critical enough to allow a precise estimation of α, the same simultaneous plus inhomogeneous consideration has been applied to the phenylene proton T_1 and $T_{1\rho}$ data reported earlier.[1] The proton data are not able to distinguish between homogeneous and inhomogeneous distributions since spin diffusion exchanges magnetization at different spatial sites. However, the overall breadth of either type of distribution is equivalently reflected in the breadth and shape of T_1 and $T_{1\rho}$ minima. The new interpretation of the proton data, including the contribution of restricted rotation, leads to an improved fit relative to the one obtained earlier with the Ngai formalism.[1] This improved analysis yields a value of 0.154 for α, and this same α is employed in the line-shape calculation. The amplitude of the restricted rotation is estimated from the high-temperature region where the flip contribution has already reached the rapid limit. We make use of the estimates reported earlier[7] based on the simultaneous model, which range in value from 64° at +120 °C to 23° at −80 °C. These estimates also prove to be effective for fitting the T_1 and $T_{1\rho}$ data where restricted rotation is included as a second motion in addition to π flips. A summary of line shape calculations at both fields is shown in Figures 3 and 4. The simulations are within the limit of experimental error. An Arrhenius analysis of τ_p's as shown in Figure 5 yields an apparent activation energy of 50 kJ/mol. Spectra at higher temperatures become rate independent for both primary and secondary processes. Simulations at temperatures beyond 0 °C are therefore not presented.

In the previous report,[1] the relaxation map log ν_c vs. T^{-1} was constructed with correlation frequencies and the corresponding temperatures for T_1 and $T_{1\rho}$ minima, average point of CSA line-shape coalescence, and maxima in dielectric and dynamic mechanical data. With the newer simultaneous-inhomogeneous description of phenylene motion, improved values of correlation frequencies for the π flips at T_1 and $T_{1\rho}$ minima and temperature for CSA collapse are obtained and used for reconstruction of the relaxation map as shown in Figure 6. The apparent activation energy (50 kJ/mol) and τ_∞ (4×10^{-17} s) obtained from linear least-squares analysis of the data are in good agreement with CSA line-shape analysis values (50 kJ/mol and 1×10^{-16} s).

The mechanical loss, $G_\gamma(\omega)^{loss}$, is given by the equation

$$G_\gamma(\omega)^{loss} = \frac{\langle \sigma_\gamma(0)^2 \rangle}{k_B T} \int_0^\infty \sin(\omega t) \phi'(t)\, dt \qquad (7)$$

where $\phi'(t)$ is the derivative of the correlation function as expressed in eq 3 and σ_γ is the stress arising from the

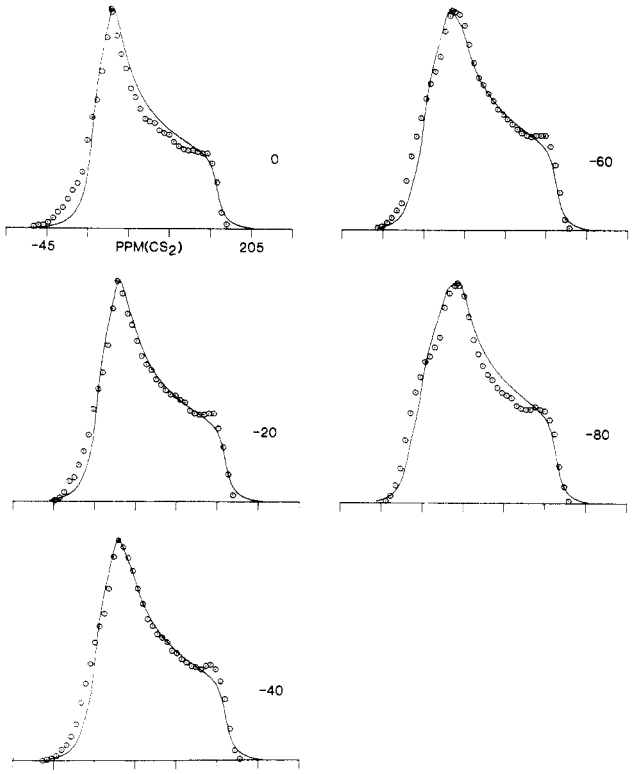

Figure 4. The solid lines are simulations of the 22.6-MHz CSA data (O) at several temperatures. The data are taken from ref 1.

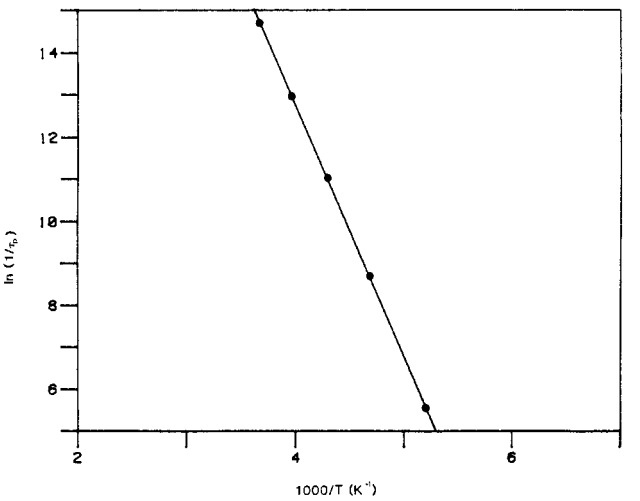

Figure 5. Logarithm of the inverse τ_p (as obtained from line-shape analysis) vs. inverse temperature.

molecular change. With this changed version of correlation function, the position and shape of the dynamic mechanical loss peaks as observed by Yee[4] were simulated by making use of eq 7, activation parameters as obtained from line-shape analysis, and an α value of 0.154. Figure 7 again shows rather good agreement between experiment and the prediction based on the interpretation of NMR data.

Discussion

In the present report, the carbon-13 CSA data base is expanded by collecting data at a higher field, i.e., 62.9 MHz, and we find the simultaneous–inhomogeneous description provides the best interpretation at both frequencies. This is a significant extension of the previous interpretation and demonstrates that NMR line-shape analysis in solids can yield a very detailed picture of the overall nature of the dynamics if a sufficiently wide data

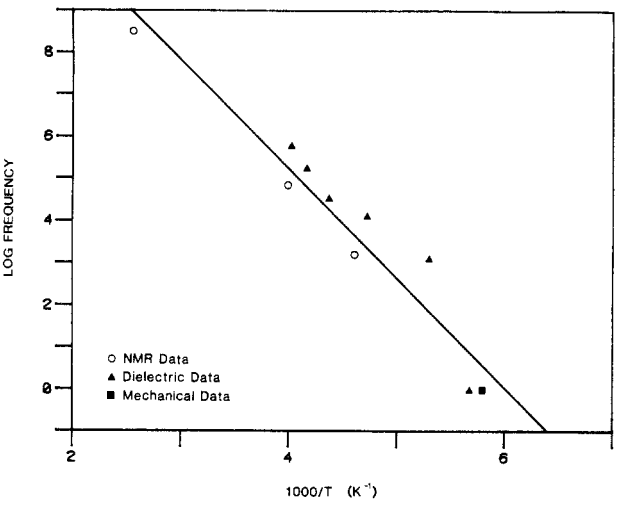

Figure 6. log (frequency) vs. inverse temperature or relaxation map. The highest frequency NMR point is the 90-MHz proton T_1 minimum, the next highest (43 kHz) is the $T_{1\rho}$ minimum, and the lowest is the average position of CSA line-shape coalescence. The filled triangles are maxima of dielectric loss curves taken at different temperatures. The positions of all points have an associated uncertainty of the order of 10 °C because of the broadness of loss peaks and relaxation minima.

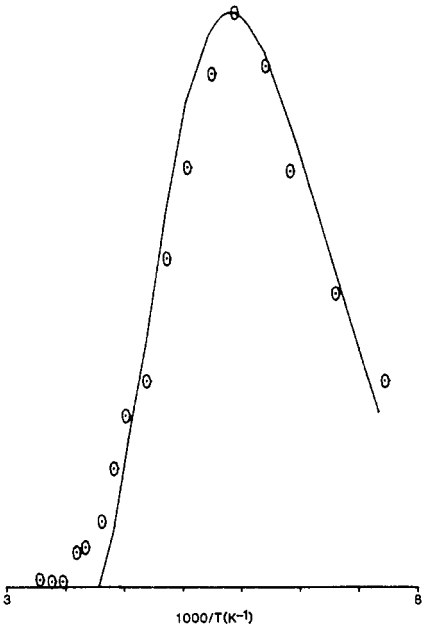

Figure 7. Dynamic mechanical spectrum. The solid line is the simulation employing the Williams–Watts inhomogeneous correlation function (eq 3) with the parameters set from the CSA line-shape analysis.

base is available. The previous estimates for the amplitude of restricted rotation or oscillation seem to be effective for fitting data at both frequencies. The primary motion includes jumps which extend over a range around exact π flips. The inhomogeneous nature of the motion indicated by the CSA spectra is plausible for a polymeric glass. Differences in packing lead to microscopic density fluctuation or a free volume distribution. Also differences in more specific interaction between chains, aside from packing effects, are also conceivable. Spatially separated groups therefore experience different barriers to motion.

The Williams–Watts formalism as expressed in eq 3 and its incorporation in multisite exchange line-shape expression represent this distribution. The breadth of the distribution may depend on the polymer structure and the nature of the motion. For BPA-PC, an α value of 0.154

indicates a broad distribution. A model[5] for motion in solid BPA-PC links the phenylene motion of the concerted cis–trans, trans–trans conformational interchange involving the carbonate unit. Since the whole process extends over more than one monomer unit, it is reasonable that the motion is more sensitive to steric hindrance and reacts to a greater degree to any density fluctuations or free volume distribution present in the system, thus yielding a broader distribution than in a case when the motion is simple and very localized.

The proposed motional model leads to the diffusion of a defect conformation along the polymer chain. The diffusing defect experiences a range of barrier heights resulting from various local packing and interaction effects and this leads to a distribution of waiting times. A diffusional process experiencing a distribution of barrier heights has been shown to lead to the stretched exponential form of correlation function.[20-22] This development from the theoretical side lends further credence to an analysis based on a Williams–Watts type correlation function.

Defect diffusion motion in combination with a distribution of barrier heights has been used to derive a stretched exponential correlation function.[20-22] However, if the distribution of barrier heights is different in the vicinity of spatially distinct relaxing groups, an inhomogeneous correlation function would result, i.e., relaxing groups at different spatial positions would have different relaxation rates. If the distribution of barriers were equivalent surrounding each spatial site, a homogeneous correlation would result. A derivation of the first case is not available, with the only derivations[20-22] corresponding to one set of barrier heights. These derivations start with a fundamentally inhomogeneous description but lead to a description of relaxation at only one site without considering the prospect of the barrier height inhomogeneity invoked, producing unequivalent relaxation at other sites.

From a general physical viewpoint, it seems unlikely that the correlation function itself is either purely inhomogeneous or purely homogeneous. The analysis considered here assumes complete inhomogeneity, and our earlier analysis,[1] complete homogeneity. The line-shape data are indicative of considerable inhomogeneity. Proton relaxation is sensitive to the presence of a distribution but cannot distinguish between homogeneous and inhomogeneous because of extensive averaging over spatial sites by spin diffusion. Carbon-13 T_1[19] and $T_{1\rho}$[11] data indicate inhomogeneous character, with spin dynamics playing a lesser role especially in the case of the T_1 data.[19] A decisive partitioning between the homogeneous and inhomogeneous aspects of relaxation in a glass which is consistent with spin–lattice relaxation and line-shape data warrants further consideration both theoretically and in the development of additional experimental data.

Temperature also affects the apparent homogeneous vs. inhomogeneous character in line-shape data. At low temperatures and intermediate exchange rates both deuterium[2] and CSA line shapes indicate an inhomogeneous distribution. However, at high temperatures, both sets of line-shape results indicate that all phenylene rings undergo large-angle flips in the fast limit. From the defect diffusion viewpoint, at lower temperature the defects can diffuse over a limited range past the lower barriers in the distribution of barrier heights. The associated rings will appear as mobile, each with its own rate. Phenylene groups experiencing high barriers will not undergo flips on the time scale of the experiment or only very slowly and will therefore appear as rigid. At high temperatures, all barriers can be surmounted in the time scale of the experiment so all rings are observed to undergo flips. If the temperature is sufficiently high, say 100 °C in BPA-PC, a distribution of flip rates still exists but all of the rates are in the fast limit, yielding the simple rapid-limit line shape, which can be simulated by any jump faster than the frequency separation of the exchanging line positions. The apparent activation energy of 50 kJ/mol, which is typical of polymeric glasses, seems quite reasonable and is in agreement with values from relaxation map analysis, mechanical data,[4] and T_1 and $T_{1\rho}$ simulations. Thus the phenomenological link in time among different NMR, dielectric, and dynamic mechanical measurements is further supported. In the same vein, the experimental data for dynamic mechanical measurements can be matched rather well, using activation parameters from line-shape analysis as input basis for eq 7, which is similarly reassuring.

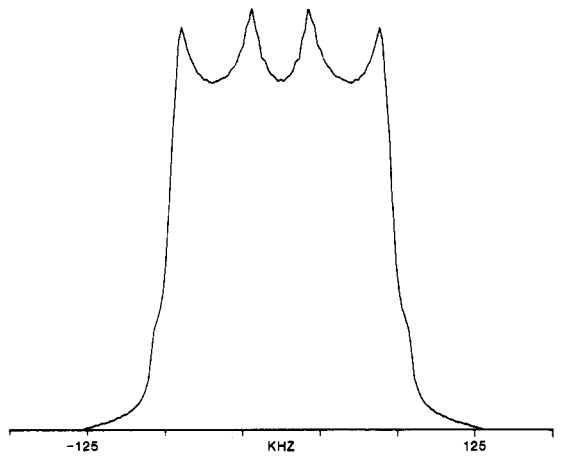

Figure 8. Theoretical deuterium spectrum, using the simultaneous–inhomogeneous description and parameters at −20 °C obtained from CSA line-shape analysis.

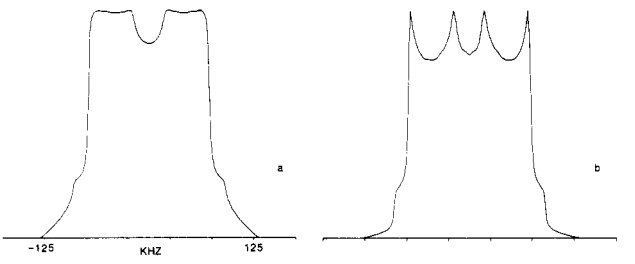

Figure 9. Comparison of homogeneous (a) and inhomogeneous (b) theoretical treatments of deuterium line shapes for phenylene group rotation for equivalent intermediate rates: (a) $\tau_p = 1.8 \times 10^{-10}$ s, $\alpha = 0.16$; (b) $\tau_p = 5.0 \times 10^{-6}$ s, $\alpha = 0.16$.

In view of the success of the simultaneous–inhomogeneous description in fitting different sets of experimental data, it seems worthwhile to generate a theoretical deuterium powder spectrum using the same motional picture and the correlation time at −20 °C. The generated spectrum should closely match the experimental deuterium spectrum at −20 °C, which has distinct features reflecting the inhomogeneous distribution.[2] Since the pulse widths and quadrupolar echo delays are not published, the corrections to the deuterium line shape cannot be affected. However, similar calculations showed that for the case of phenylene flipping, incorporating the corrections shifts the correlation times by a certain factor, but the basic line-shape features remain. Figure 8 shows the calculated line shape, which displays the same general features as the −20 °C expermental spectrum. This similarity in line shape obtained with the correlation time at −20 °C from CSA

line-shape analysis gives additional confidence in the phenylene dynamics picture as outlined here. It should be noted that due to the increased quadrupolar interaction, the features that distinguish homogeneous and inhomogeneous line shapes for intermediate rates, i.e., the differences at the absorption maxima, are enhanced over the CSA case as shown in Figure 9.

Acknowledgment. This research was carried out with the financial support of National Science Foundation Grant DMR-790677, of National Science Foundation Equipment Grant No. CHE 77-09059, of National Science Foundation Grant No. DMR-8018679, and of U.S. Army Research Office Grants DAAG 29-82-G-0001 and DAAG 29 85-K0126.

Registry No. BPA-PC (copolymer), 25037-45-0; BPA-PC (SRU), 24936-68-3.

References and Notes

(1) O'Gara, J. F.; Jones, A. A.; Hung, C.-C.; Inglefield, P. T. *Macromolecules* **1985**, *18*, 1117.
(2) Spiess, H. W. *Advances in Polymer Science*; Kausch, H. H., Zachmann, H. G., Eds.; Springer-Verlag: Berlin, 1984.
(3) (a) Illers, K.; Bruer, H. *Kolloid-Z.* **1961**, *176*, 110. (b) Krum, F.; Muller, F. H. *Kolloid-Z.* **1957**, *164*, 81. (c) Krum, F. *Kolloid-Z.* **1959**, *165*, 77.
(4) Yee, A. F.; Smith, S. A. *Macromolecules* **1981**, *14*, 54.
(5) Jones, A. A. *Macromolecules* **1985**, *18*, 902.
(6) Wemmer, D. E. Ph.D. Thesis, University of California, Berkeley, CA, 1979.
(7) Roy, A. K.; Jones, A. A.; Inglefield, P. T. *J. Magn. Reson.* **1985**, *64*, 441.
(8) Ngai, K. L. *Comments Solid State Phys.* **1979**, *9*, 127.
(9) Ngai, K. L.; White, C. T. *Phys. Rev. B* **1979**, *20*, 2476.
(10) Ngai, K. L. *Phys. Rev. B* **1980**, *22*, 2066.
(11) (a) Schaefer, J.; Stejskal, E. O.; Steger, T. R.; Sefcik, M. D.; McKay, R. A. *Macromolecules* **1980**, *13*, 1121. (b) Steger, T. R.; Schaefer, J.; Stejskal, E. O.; McKay, R. A. *Macromolecules* **1980**, *13*, 1127.
(12) Kaplan, J. I.; Garroway, A. N. *J. Magn. Reson.* **1982**, *49*, 464.
(13) Mehring, M. *High Resolution NMR in Solids*, 2nd ed.; Springer-Verlag: New York, 1983.
(14) Bloembergen, N.; Rowland, T. J. *Acta Metall.* **1955**, *1*, 731.
(15) Wemmer, D. E.; Ruben, D. J.; Pines, A. *J. Am. Chem. Soc.* **1981**, *103*, 28.
(16) Williams, G.; Watts, D. C. *Trans. Faraday Soc.* **1970**, *66*, 80.
(17) Montroll, E. W.; Bendler, J. T. *J. Stat. Phys.* **1984**, *34*, 129.
(18) Bendler, J. T.; Shlesinger, M. F. In *Studies in Statistical Mechanics*; Shlesinger, M. F., Weiss, G. H., Eds.; North-Holland: New York, 1985; Vol. 12.
(19) Connolly, J.; Jones, A. A.; Inglefield, P. T., to be published.
(20) Shlesinger, M. F.; Montroll, E. W. *Proc. Natl. Acad. Sci. U.S.A.* **1984**, *81*, 1280.
(21) Shlesinger, M. F. *J. Stat. Phys.* **1984**, *36*, 639.
(22) Blumen, A.; Zumofen, G.; Klafter, J. *Phys. Rev. B* **1984**, *30*, 5379.

Surface Structure and Oxygen Permeation in Mixed Multibilayer Films of Hydrocarbon and Fluorocarbon Amphiphiles

Nobuyuki Higashi,† Toyoki Kunitake,*† and Tisato Kajiyama‡

Department of Organic Synthesis and Department of Applied Chemistry, Faculty of Engineering, Kyushu University, Fukuoka 812, Japan. *Received August 29, 1985*

ABSTRACT: Multicomponent bilayers of double-chain (fluorocarbon, 2F; hydrocarbon, 2H; mixed chain, 1F1H) ammonium amphiphiles were immobilized on Millipore membranes as composite films with poly(vinyl alcohol). Differential scanning calorimetry and ESCA indicated that the hydrocarbon and fluorocarbon components form separated domains and that the fluorocarbon component is concentrated near the film surface. Permeation of O_2 and N_2 through these films was examined by the high-vacuum method. The separation factor (P_{O_2}/P_{N_2} = 2.0–2.8) was apparently determined by the surface monolayer formed from the fluorocarbon (2F) amphiphile, without regard to the hydrocarbon (2H) content. The permeability coefficient (P) was enhanced by the presence of the fluid domain of the liquid-crystalline hydrocarbon (2H) bilayer, and a 100 times jump in P was observed for a composite film of 2F/2H/1F1H (1:7:1) and PVA near the phase transition temperature of the hydrocarbon bilayer.

Introduction

Aqueous bilayer membranes can be immobilized by casting on glass in the form of transparent films that maintain the bilayer characteristics.[1-4] Fluorocarbon bilayer films obtained by casting with and without poly(vinyl alcohol) (PVA) exhibit the oxygen-enrichment property.[5] Takahara et al.[6] conducted the structural characterization of composite films of PVA and fluorocarbon bilayer membranes by X-ray diffraction and X-ray photoelectron spectroscopy (XPS) and discovered that the fluorocarbon bilayer lamella is spontaneously concentrated at the film surface with the bilayer orientation parallel to the film plane.

In general, permeability coefficients of the bilayer membrane are enhanced when the bilayer membrane is in the liquid-crystalline phase rather than in the crystalline phase. Fluorocarbon bilayer films show enhanced oxygen permeation due to the affinity between fluorocarbon moieties and molecular oxygen. In contrast, fluorocarbon bilayers possess high phase transition temperatures (T_c), and the enhanced permeation due to the liquid-crystalline state cannot be achieved at ambient temperatures. We

Chart I

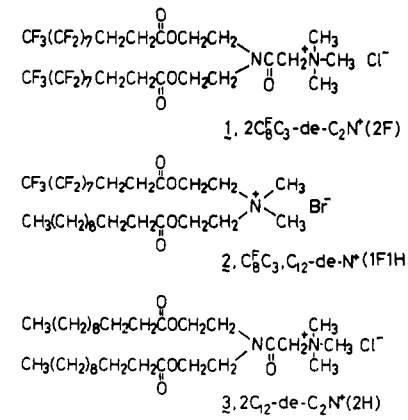

† Department of Organic Synthesis, Contribution No. 804.
‡ Department of Applied Chemistry.

0024-9297/86/2219-1362$01.50/0